A hybrid simulated method for analyzing the optical efficiency of a head-mounted display with a quasi-crystal OLED panel

Kao-Der Chang,[1] Chang-Yi Li,[2] Jui-Wen Pan,[2,3,4,*] and Kuei-Yuan Cheng[1]

[1] *Mechanical and Systems Research Laboratories, Industrial Technology Research Institute of Taiwan, Hsin-Chu City 31040, Taiwan*

[2] *Institute of Photonic System, National Chiao Tung University, Tainan City 71150, Taiwan*

[3] *Biomedical Electronics Translational Research Center, National Chiao Tung University, Hsin-Chu City 30010, Taiwan*

[4] *Department of Medical Research, Chi Mei Medical Center, Tainan City 71004, Taiwan*

**juiwenpan@gmail.com*

Abstract: Organic light emitting diodes (OLEDs) with a quasi-crystal (QC) structure are analyzed and applied in a head-mounted display (HMD) system in this study. We adopt a hybrid simulated method to evaluate the light extraction efficiency (LEE) and far-field pattern in the air, and study the relationship between them. The simulation results show that OLEDs implanted with the QC structure can provide a collimated far-field pattern to increase the brightness. Using this 10-fold QC arrangement the maxima LEE of the OLEDs can be increased by 1.20 times. Compared with conventional OLEDs, the viewing angle of the OLED panel decreases from 120 degrees to 26 degrees with an improvement in the optical efficiency of the HMD system by 2.66 times. Moreover, the normalized on-axis intensity in the pupil of the eyepiece can be enlarged up to 3.95 times which suggests that the OLED panel can save 74.68% energy while achieving the same on-axis intensity as conventional OLEDs.

OCIS codes: (050.5298) Photonic crystals; (250.3680) Light-emitting polymers; (120.2820) Heads-up displays.

References and links

1. S. Kunić and Z. Šego, "OLED Technology and Display," Int. Symp. ELMAR, 37–40 (2012).
2. C. H. Oh, H. J. Shin, W. J. Nam, B. C. Ahn, S. Y. Cha, and S. D. Yeo, "Technological Progress and Commercialization of OLED TV," SID Int. Symp. Dig. Tech. Pap. **44**(1), 239–242 (2013).
3. Website: http://www.emagin.com/
4. D. Kessler and M. Bablani, "Head-mounted optical apparatus using an OLED display," U.S. patent 8094377 B2 (Jan. 10, 2012).
5. J. K. Borchardt, "Developments in organic displays," Mater. Today **7**(9), 42–46 (2004).
6. S. Nowy, B. C. Krummacher, J. Frischeisen, N. A. Reinke, and W. Brutting, "Light extraction and optical loss mechanisms in organic light-emitting diodes: Influence of the emitter quantum efficiency," J. Appl. Phys. **104**(12), 123109 (2008).
7. Y. Sun, N. C. Giebink, H. Kanno, B. Ma, M. E. Thompson, and S. R. Forrest, "Management of singlet and triplet excitons for efficient white organic light-emitting devices," Nature **440**(7086), 908–912 (2006).
8. K. Saxena, V. K. Jain, and D. S. Mehta, "A review on the light extraction techniques in organic electroluminescent devices," Opt. Mater. **32**(1), 221–233 (2009).
9. J. Zhou, N. Ai, L. Wang, H. Zheng, C. Luo, Z. Jiang, S. Yu, Y. Cao, and J. Wang, "Roughening the white OLED substrate's surface through sandblasting to improve the external quantum efficiency," Org. Electron. **12**(4), 648–653 (2011).
10. N. Nakamura, N. Fukumoto, F. Sinapi, N. Wada, Y. Aoki, and K. Maeda, "Glass Substrates for OLED Lighting with High Out-coupling Efficiency," J. Soc. Inf. Disp. **40**(1), 603–606 (2009).
11. U. Geyer, J. Hauss, B. Riedel, S. Gleiss, U. Lemmer, and M. Gerken, "Large-scale patterning of indium tin oxide electrodes for guided mode extraction from organic light-emitting diodes," J. Appl. Phys. **104**(9), 093111 (2008).
12. J. Hauss, T. Bocksrocker, B. Riedel, U. Lemmer, and M. Gerken, "On the interplay of waveguide modes and leaky modes in corrugated OLEDs," Opt. Express **19**(S4), A851–A858 (2011).

#203728 - $15.00 USD Received 26 Dec 2013; accepted 18 Feb 2014; published 10 Mar 2014

13. Y. R. Do, Y. C. Kim, Y. W. Song, and Y. H. Lee, "Enhanced light extraction efficiency from organic light emitting diodes by insertion of a two-dimensional photonic crystal structure," J. Appl. Phys. **96**(12), 7629 (2004).
14. R. Yan and Q. Wang, "Enhancement of light extraction efficiency in OLED with two-dimensional photonic crystal slabs," Chin. Opt. Lett. **4**(6), 353–356 (2006).
15. Y. J. Lee, S. H. Kim, J. Huh, G. H. Kim, Y. H. Lee, S. H. Cho, Y. C. Kim, and Y. R. Do, "A high-extraction-efficiency nanopatterned organic light-emitting diode," Appl. Phys. Lett. **82**(21), 3779 (2003).
16. W. Xu and Y. Li, "The Effect of Anisotropy on Light Extraction of Organic Light-Emitting Diodes with Photonic with Photonic Crystal Structure," J. Nanomater. **2013**, 969120 (2013).
17. Y. J. Lee, S. H. Kim, G. H. Kim, Y. H. Lee, S. H. Cho, Y. W. Song, Y. C. Kim, and Y. R. Do, "Far-field radiation of photonic crystal organic light-emitting diode," Opt. Express **13**(15), 5864–5870 (2005).
18. S. Jeon, J. W. Kang, H. D. Park, J. J. Kim, J. R. Youn, J. Shim, D. G. Choi, K. D. Kim, A. O. Altun, S. H. Kim, and Y. H. Lee, "Ultraviolet nanoimprinted polymer nanostructure for organic light emitting diode application," Appl. Phys. Lett. **92**(22), 223307 (2008).
19. S. S. Jeong and J. H. Ko, "Optical Simulation Study on Effect of Diffusing Substrate and Pillow Lenses on the Outcoupling Efficiency of Organic Light Emitting Diodes," J. Opt. Soc. Kor. **17**(3), 269–274 (2013).
20. A. Taflove and S. C. Hagness, *Computational Electrodynamics: The Finite-Difference Time-Domain Method*, 2nd ed. (Artech House, 2000).
21. Website: http://optics.synopsys.com/lighttools/
22. P. W. Zhai, Y. K. Lee, G. W. Kattawar, and P. Yang, "Implementing the near- to far-field transformation in the finite-difference time-domain method," Appl. Opt. **43**(18), 3738–3746 (2004).
23. Website: http://docs.lumerical.com/en/fdtd/user_guide_changing_the_far_field_index.html
24. A. Chutinan, K. Ishihara, T. Asano, M. Fujita, and S. Noda, "Theoretical analysis on light extraction efficiency of organic light-emitting diodes using FDTD and mode-expansion methods," Org. Electron. **6**(1), 3–9 (2005).
25. Website: http://www.emagin.com/wp-content/uploads/2010/08/SVGA_Rev3_XL_User_Manual_Datasheet_Rev_41.pdf
26. L. Jia, I. Bita, and E. L. Thomas, "Photonic density of states of two-dimensional quasicrystalline photonic structures," Phys. Rev. A **84**(2), 023831 (2011).
27. A. Ricciardi, I. Gallina, S. Campopiano, G. Castaldi, M. Pisco, V. Galdi, and A. Cusano, "Guided resonances in photonic quasicrystals," Opt. Express **17**(8), 6335–6346 (2009).
28. S. Matloub, M. Noori, and A. Rostami, "Reduction of guided waves in ITO/glass interface of white organic light emitting diodes (WOLEDs): Layer optimization," Optik (Stuttg.) **124**(21), 5061–5063 (2013).
29. H. Peng, Y. L. Ho, X. J. Yu, M. Wong, and H. S. Kwork, "Coupling efficiency enhancement in organic light-emitting devices using microlens array-theory and experiment," J. Display Technol. **1**(2), 278–282 (2005).
30. K. Y. Chen, Y. T. Chang, Y. H. Ho, H. Y. Lin, J. H. Lee, and M. K. Wei, "Emitter apodization dependent angular luminance enhancement of microlens-array film attached organic light-emitting devices," Opt. Express **18**(4), 3238–3243 (2010).
31. ZEBASE Optical Design Database user's Guide Version 6.0. (2007), p. 50.
32. W. J. Smith, "Eyepiece and Magnifiers," in *Modern Lens Design*, 2nd ed. (Mc-Graw Hill, 2005), pp. 151–152.
33. D. Armitage, I. Underwood, and S.-T. Wu, "Near-to-Eye Systems," in *Introduction to Microdisplays* (John Wiley, 2006), pp. 341–342.
34. W. J. Smith, *Modern Optical Engineering* (Mc Graw Hill, 2008), pp. 160–161.

1. Introduction

Organic light-emitting diodes (OLEDs) have found major application because they can provide high brightness, quick response time, low power consumption and superior color rendering [1]. On the basis of these excellent characteristics, OLEDs have attracted much attention for use in displays and general lighting during in recent decades. In addition to the implementation of OLEDs in large-size flat panel displays (FPD) [2], they have also been used in small-screen devices such as smart phones and head-mounted displays (HMD) due to their self-luminescence, light weight and thin thickness [3]. The optical system for a HMD system with liquid crystal on silicon (LCoS) panels consists of an illumination system and image system. The LCoS panel is not a light emitting source so an additional illumination system is needed to light up the LCoS panel. For portable applications requiring compact size and light weight, it is necessary to replace the LcoS with the OLED panel in the HMD system [4]. Although they are more suitable for portable display devices [5], the light extraction efficiency (LEE) of the conventional OLED is still poor (~20%) [6]. The brightness is not enough for the human eye due to the influence of ambient light. In addition, the wide intensity distribution of the far-field pattern is another disadvantage for this kind of display application. To meet the above needs, the current research is dedicated to not only to improving the

#203728 - $15.00 USD Received 26 Dec 2013; accepted 18 Feb 2014; published 10 Mar 2014

optical efficiency of OLEDs but also to take improving the far-field pattern into consideration.

Nowadays, the internal quantum efficiency of OLEDs can reach 100% by using phosphorescent emitters [7]. However, the total internal reflection (TIR) in high refractive index layers results in LEE deficiency. There is an extensive body of literature dealing with enhancing the external quantum efficiency of OLEDs [8] and there have been numerous studies about increasing the LEE. The related works can be classified into several areas: roughening [9], scattering layers [10], gratings [11], and one- and two-dimensional photonic crystals (PCs). According to past work, utilizing the photonic crystals is a desirable method to improve the LEE of OLEDs. The structure of the photonic crystals can be coupled with the waveguide mode which is trapped in the high refractive index layers to leaky modes [12]. The square lattice PCs embedded between the indium tin oxide (ITO) layer and the substrate effectively allow the trapped light to escape from the ITO layer [13]. Similar approaches have been taken to address the LEE of OLEDs devices [14,15]. Owing to the periodic structure, the intensity distribution of the light extraction is obvious in the far-field pattern [16,17]. This reveals that the diffraction phenomenon is important when periodic PCs are introduced into OLEDs. For an HMD system with an OLED panel, the rays emitted from the OLED panel pass through the eyepiece to generate an image on the human eye. The aperture of the eyepiece limits the cone angle of the OLED panel which means that photonic crystal OLEDs which have the property of a wide intensity distribution are inappropriate to employ as the illumination light source in the HMD system. Therefore, we utilize quasi-crystal structure embedded in the OLEDs to ameliorate the problem with the intensity distribution. Furthermore, the enhancement of the LEE and the relations corresponding to the intensity distribution are considered at the same time.

In this investigation, we utilize 2D quasi-crystal (QC) structure which is sandwiched between a glass substrate and the ITO. A SiNx buffer layer is inserted underneath the ITO to smooth the ITO/HTL interface [18]. The functioning of the actual HMD system with the OLED panels is estimated with a hybrid method which combines the finite-difference time-domain (FDTD) and ray-tracing method [19–21]. The Lumerical FDTD Solutions and LightTools software correspond to the wave and ray methods, respectively. In this study, we find that OLED implanted QC structures give collimated far-field patterns. Furthermore, the optical efficiency of the HMD system can be evaluated by adopting this hybrid method and the performance of the system is also discussed and compared the performance of the QC-based HMD system. The results show that the viewing angle of the QC-based HMD can be adjusted from 120 degrees to 26 degrees and the enhancement of optical efficiency can be improved up to 2.66 times. Overall, the normalized on-axis intensity of the pupil of the eyepiece can be enlarge up to 3.95 times which suggests that the OLED panel can offer an energy saving of 74.68% while achieving the same on-axis intensity as conventional OLEDs.

2. Design of the flow chart and the bottom emitting OLED structure

2.1 Simulation flow chart

In wave optics, the near-field means that the emitted wavelength and the propagating distance are of the same order. If the propagating distance is much greater than the emitted wavelength, it is called the far-field. In general, OLEDs are only a few micrometers thick, which is easy to simulate in the near-field using the FDTD method. However, the thickness of the covering glass of the OLEDs is too thick to calculate using the same method, failing to obtain the radiated power in air in the far-field directly. Hence, the OLED simulation method must be rethought. To overcome this disadvantage, a hybrid method combining the wave method with the ray method is used. The simulation flow chart is shown in Fig. 1. First of all, the near-field information for an OLED implanted PC structure can be calculated via the FDTD method. By combining the Near-to-Far-Field transformation (NTFF) method [22] with

#203728 - $15.00 USD Received 26 Dec 2013; accepted 18 Feb 2014; published 10 Mar 2014

Fresnel correction [23], the LEE and the far-field pattern of OLEDs in air can be obtained. Following the FDTD simulation, the far-field pattern in air can be processed and transferred into angular space through ray optics. The whole optical system with the OLEDs and the HMD system can be estimated with the ray-tracing method. Using this hybrid method, the wave and ray results for the OLEDs can be analyzed in greater detail and with more freedom. Through the hybrid method, the far-field pattern in air can be utilized in the HMD system for evaluating the optical efficiency.

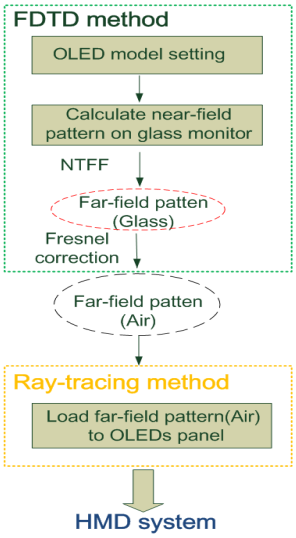

Fig. 1. Simulation flow chart for the hybrid method.

2.2 Architecture of the FDTD simulation

As can be seen in the flow chart above, information about the OLEDs in the near-field can be obtained by the FDTD simulation. Owing to the limitations of computer member for the FDTD method, the size of the OLEDs is restricted to $8x8x2\mu m^3$. Perfect match layers (PML) are placed on all sides. The structures of the conventional OLEDs and PC-based OLEDs are shown in Fig. 2. The conventional OLED structure consists of a metal cathode, an electron transport layer (ETL), a hole transport layer (HTL), a ITO and a glass substrate. In the PC-based OLEDs, the PC structures are sandwiched between the glass substrate and the ITO. A SiNx buffer layer is inserted under the ITO to smooth the ITO/HTL interface. It is assumed that the dipoles are emitted at the interface of the ETL and HTL. The excited dipoles have polarizations along the x, y and z directions to represent the arbitrary directions of the dipole. The estimation results can be obtained by averaging over all dipole directions [24]. To ensure stable conditions, the simulated time step is 0.01 fs and 10000 FDTD time steps are iterated. The spatial resolution is set below 6nm corresponding to the refractive index of the material and the thickness of the layer.

#203728 - $15.00 USD Received 26 Dec 2013; accepted 18 Feb 2014; published 10 Mar 2014

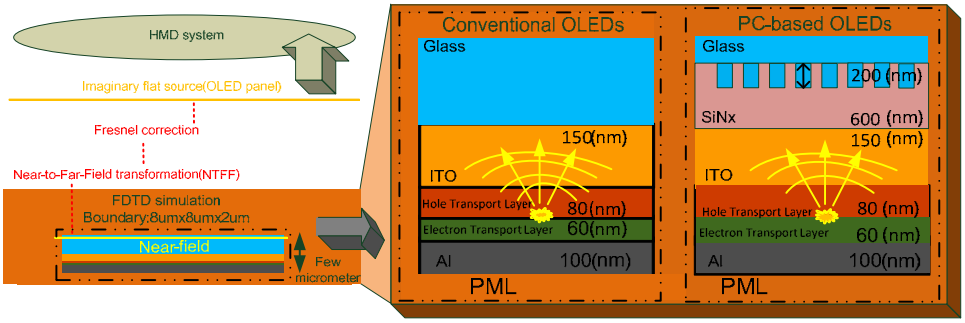

Fig. 2. Optical configuration of the OLEDs and the HMD system. The left-hand figure illustrated the hybrid method developed for connecting and evaluating the optical configuration. The right-hand figure shows the conventional OLED and the PC-based OLEDs. The thickness of the Al, electron transport layer, hole transport layer, ITO, SiNx, and the height of the PCs are 100 nm, 60 nm, 80 nm, 150 nm, 600 nm and 200 nm, respectively.

2.3 Architecture of the ray-tracing simulation

The thickness of the glass makes simulation difficult using only the FDTD method, therefore it is necessary to combine it with the NTFF method and the Fresnel correction method, as shown in Fig. 2. In this way, the far-field pattern for OLEDs in air can be obtained from the FDTD. The whole optical system containing OLEDs and the HMD system can be estimated by adopting the ray-tracing method. In order to connect with the HMD system, the raw data for the far-field pattern can be processed and modified using the ray-tracing software (LightTools). The far-field pattern in air represents an imaginary flat source which has the same intensity distribution as air. The intensity distribution of this flat source is imported by processing the far-field pattern in air. The spatial distribution is arranged for an OLED panel with a resolution of 852x600 [25]. Through the above arrangement and procedure, the far-field in air can be utilized to simulate and link the HMD system. The optical efficiency and view angle of the whole system can be estimated systematically.

3. Simulation analysis

3.1 Different arrangements of two-dimensional photonic-crystals (PCs) and quasi-crystals (QCs)

The influence of the PC structure is analyzed after inserting two-dimensional PCs into the SiNx layer between the ITO and the glass layer. The crystal structures can include rectangular, hexagonal, 8-fold, 10-fold and 12-fold QCs. The multi-fold construction of the QCs is described with Eq. (1) [26–28]. The variable n_{fold} indicates the rotational symmetry of the associated QCs and the lattice constant of n_{fold} is represented by a. Following this assumption, the two-dimensional morphologies of the QCs established in this study can be evaluated.

$$f(x,y)=\sum_{n=0}^{n_{fold}/2-1}\cos[2\pi x\cos(2\pi n/n_{fold})/a+2\pi y\sin(2\pi n/n_{fold})/a] \quad (1)$$

Figure 3 illustrates the OLED structure implanted with 10-fold QCs, where the right-hand figure represents the top view of the 10-fold QCs. The dielectric glass rod is embedded in the SiNx layer. To simplify, the filling factor (radius/lattice constant) and depth of the patterns are chosen to be 0.5 and 200 nm, respectively. The same assumption is also suitable for rectangular, hexagonal and other multi-fold QCs.

#203728 - $15.00 USD Received 26 Dec 2013; accepted 18 Feb 2014; published 10 Mar 2014

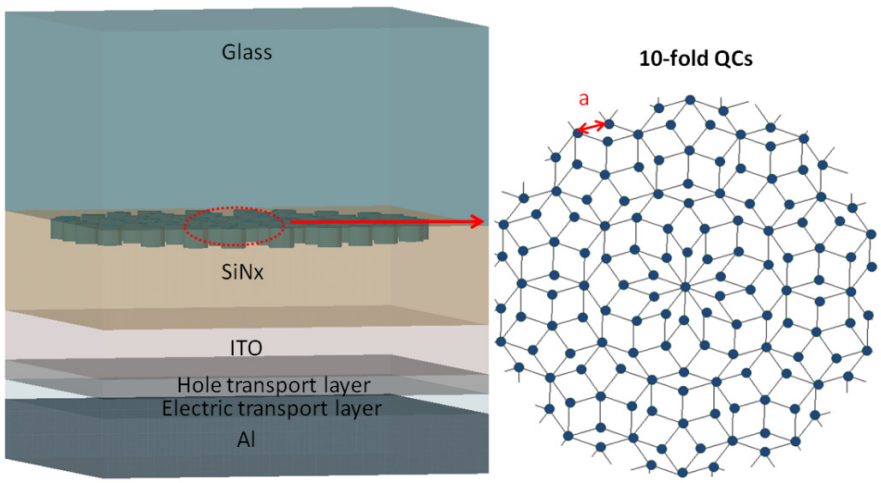

Fig. 3. The 3D layout of a 10-fold QC OLED with a glass dielectric rod embedded in the SiNx layer. The right-hand figure shows the top view of a 10-fold QC arrangement with a lattice constant of a.

3.2 FDTD analysis

The LEE of the different arrangements is analyzed, the enhancement of LEE is defined as in Eq. (2), where P is the Poynting vector of the far-field pattern when the near-field is projected by the distances of R. P_{Con} and P_{Des} are corresponding to the Poynting vector of conventional OLEDs (without structure) and PC-based OLEDs (with structure). By integrating the Poynting vector with all angles and wavelengths ranging from 400nm to 700nm, the enhancement of LEE in the different designed structures can be evaluated, where enhancement factor is represented by EF.

$$EF = \frac{\int_{400}^{700} \iint \vec{P}_{Des}(\theta,\varphi,\lambda) R^2 \sin(\theta) d\theta d\varphi d\lambda}{\int_{400}^{700} \iint \vec{P}_{Con}(\theta,\varphi,\lambda) R^2 \sin(\theta) d\theta d\varphi d\lambda}, R \geq 1mm \quad (2)$$

To simplify, the parameters (as shown in Fig. 2) are fixed, except for the lattice constant. The results of a comparison of the different structures are plotted in Fig. 4. The lattice constant varies from 200nm to 1000nm. The conventional OLED is represented at the condition with a lattice constant of 0 nm. With an increase in the lattice constant, the enhancement of the LEE in air can be achieved, as shown in Fig. 4(a). Examination of the different structural morphologies shows that the 10-fold QC demonstrated better performance than the other arrangements. With the 10-fold QC structure there is an improvement in the maximum LEE of 1.2 times when the lattice constant is 800 nm. For larger lattice constants, there is a similar decline in the enhancement of the LEE for the different structures due to the scattering effect from the diffraction of the light. The far-field patterns in air with different QCs obtained by adopting the NTFF method and the Fresnel correction are illustrated in Fig. 4(b). The distribution of far-field patterns is observed for various different lattice constants: 0 nm, 500 nm and 800 nm. From the calculated results, we find that the far-field pattern has collimated distribution when the lattice constant is 500 nm. When the lattice constant is 800 nm, the far-field pattern has a batwing distribution corresponding to the maximum LEE. In addition, the diffraction phenomenon is obvious in the 8-fold and 12-fold QCs. The explanation for the results may be that the light diffraction suppressed the LEE in the OLEDs, and therefore the 10-fold QCs showed better performance than the other QCs.

#203728 - $15.00 USD Received 26 Dec 2013; accepted 18 Feb 2014; published 10 Mar 2014

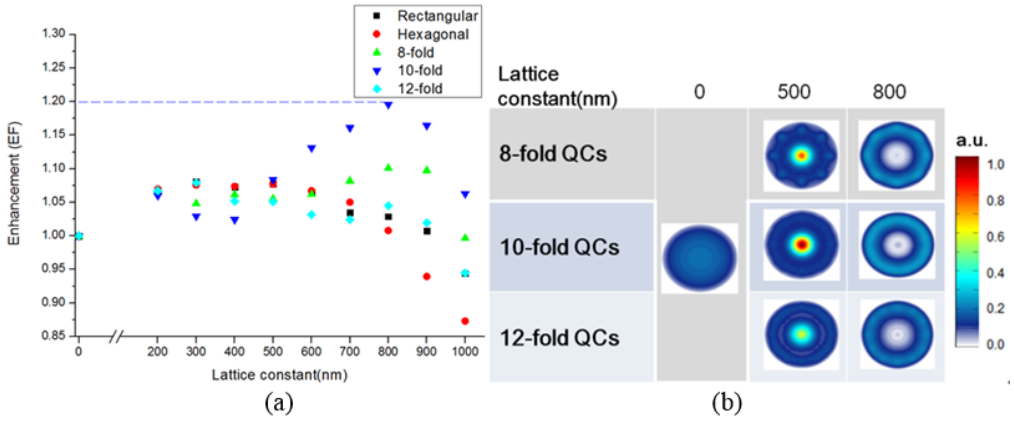

Fig. 4. (a) The enhancement of LEE as a function of the lattice constant and the arrangement in the air. (b) The far-field pattern with QCs in air at a lattice constant of 0 nm, 500 nm or 800 nm, respectively.

3.3 Comparison of ray-tracing analysis and FDTD method results in air

The radiated power of the OLED panel in air can be obtained by using the FDTD method directly with Fresnel correction, but the boundary effect of the glass layer is not considered. In order to examine the disparity, we combine the NTFF results for the glass layer with those from the ray-tracing method in the actual size of OLEDs. A similar method has been reported for evaluating the performance of OLEDs with an optimal microlens array [29,30]. In the simulation, a 10-fold QC OLED structure is used with the same parameters as those mentioned above. In the ray tracing method with the NTFF results for the glass not only is the Fresnel correction considered but also the influence of the intercept with the boundary. The estimation results associated with various lattice constant are shown in Fig. 5.

From the ray-tracing method for the actual size of the OLEDs, it can be seen that the maximum LEE enhancement is 1.23 times with lattice constant of 800 nm. In comparison, with the FDTD method, the maximum LEE enhancement is 1.20 times for the same lattice constant. The LEE enhancement is slightly higher when the lattice constant ranges from 400 nm to 1000 nm according to the ray-tracing method and the actual size of OLEDs. This result indicates that the multiple reflections affect the enhancement of the LEE. On the whole, the maximum deviation between the two methods is 2.5% which is in within the reasonable range and the tendency of the calculated results is consistent. Since the primary concern is the optical efficiency of the whole system, the FDTD method with Fresnel correction is appropriate for reducing the complexity of the simulation procedure. In the next section, we discuss the application of the far-field pattern from the FDTD method with Fresnel correction for an HMD system and evaluate the corresponding enhancement of optical efficiency.

#203728 - $15.00 USD Received 26 Dec 2013; accepted 18 Feb 2014; published 10 Mar 2014

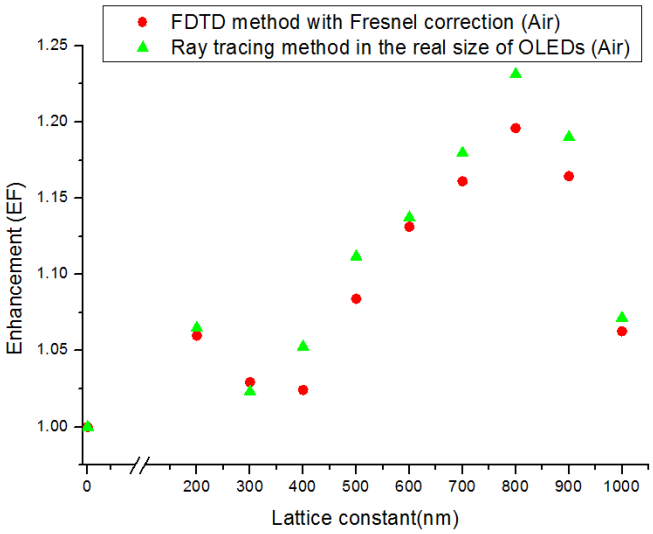

Fig. 5. Comparison of the results obtained with two different simulation methods. The relationships between the enhancement of the 10-fold QCs for the different lattice constants show that a maximum deviation of 2.5% which is within the reasonable range and the tendency of the calculated results are consistent.

3.4 Comparison of the eyepiece system

The imaging system for the HMD system is a typical eyepiece lens. A symmetrical eyepiece is chosen from among four-element eyepieces for baseline comparison [31], as shown in Fig. 6(a). The panel area of the OLED is 12.78mm x 9mm, the diagonal field of view is designed to be 30 degrees and the pupil of the eyepiece has a diameter of 8 mm [32,33].

As mentioned in the preceding section, there are three kinds of far-field patterns for the application of OLEDs in an HMD system. In the 1st pattern the lattice constant is 0 nm (conventional OLEDs). The full width at half maximum (FWHM) of the intensity distribution is 120 degrees with a Lambertian distribution. In the 2nd pattern, the maximum LEE occurs with a lattice constant of 800 nm. The intensity distribution of the 2nd pattern is a batwing distribution. The maximum intensity occurs at 49 degrees. For the comparison of different intensity distributions, the collimated far-field pattern of the OLEDs is chosen for comparison. The collimated far-field pattern occurs with a lattice constant of 500 nm. The FWHM for the intensity distribution can reach 26 degrees. The intensity distribution with the lattice constant of 500 nm is chosen as the 3rd pattern. The intensity distributions of the three different kinds of far-field patterns are shown in Fig. 6(b).

The on-axis intensity and the enhancement of optical efficiency of the HMD system can be compared through examination of the three normalized intensity distributions for the pupil of the eyepiece shown in Fig. 6(c). The normal intensity is set by the on-axis intensity of the 1st pattern for three intensity distributions. Among the three kinds of far field patterns, there is an increase in the normalized on-axis intensity of 3.95 times for the 3rd pattern, but a reduction in the normalized on-axis intensity to 0.16 times for the 2nd pattern. Therefore, the collimation of the three kinds of far-field patterns will take effect with the normalized on-axis intensity. Furthermore, the optical efficiency can be obtained by integrating the normalized intensity distribution. Comparison shows a substantial enhancement in the optical efficiency of the HMD system of 2.66 times with the 3rd pattern. In contrast, there is a reduction in the optical efficiency of 0.30 times with the 2nd pattern. The results of the comparison of these phenomena are shown in Table 1.

#203728 - $15.00 USD Received 26 Dec 2013; accepted 18 Feb 2014; published 10 Mar 2014

$$\gamma(\%) = (1 - \frac{\beta}{\alpha}) \times 100\% \quad (3)$$

Owing to the characteristics of the human eye, the maximum visual acuity (VA) is at the normal direction of the human eye [34]. The intensity at the normal direction is thus chosen for comparison. For the purpose of the energy conservation, the power saving can be defined as in Eq. (3), where γ is the ratio of the power saving. At the pupil of eyepiece, β is the normalized on-axis intensity of the conventional OLEDs and α is represented as normalized on-axis intensity of input far-field pattern. The results of the calculation for three patterns are shown in Table 1. In one word, these results of the simulation indicate that the main intensity distribution of the 2nd pattern is located at a larger angle, so that the normalized on-axis intensity at the pupil of the eyepiece is the lowest among three patterns. Thus, the collimation level and the FWHM of the intensity distribution with the OLED panel are significant factors in the HMD system.

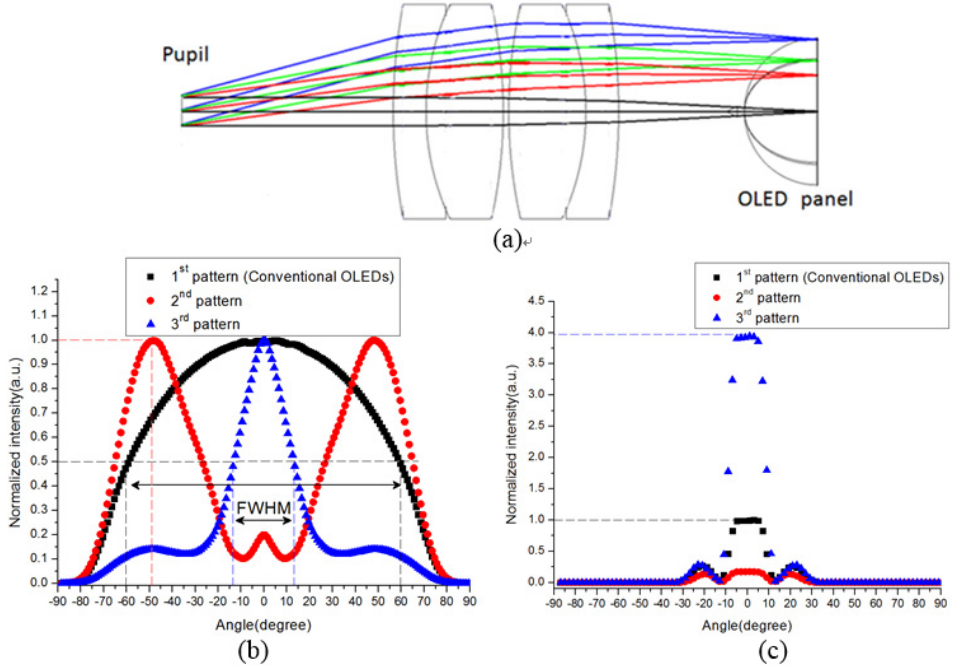

Fig. 6. (a) The layout of the eyepiece, (b) relationship between normalized intensity distributions for the OLED panel, (c) and the normalized intensity distribution for the pupil of the eyepiece.

Table 1. Comparison of three far-field patters in the HMD system

Input far-field pattern	1st pattern (Conventional OLEDs)	2nd pattern	3rd pattern
Normalized enhancement of optical efficiency	1	0.30	2.66
Normalized on-axis intensity	1	0.16	3.95
Power saving (%)	0%	–525%	74.68%

#203728 - $15.00 USD Received 26 Dec 2013; accepted 18 Feb 2014; published 10 Mar 2014

4. Conclusion

The enhancement of optical efficiency and the on-axis intensity in an HMD system with OLED plane implanted QCs are evaluated using a hybrid method which includes the FDTD and ray-tracing simulation. Five arrangements are considered and the results suggest that greater improvement of the LEE can be achieved with 10-fold QCs than with other structures for lattice constant ranging from 500 nm to 1000 nm. In particular, there is a maximum 1.2 time enhancement of the LEE when the lattice constant is 800 nm. However, it is found that a 10-fold QC with a lattice constant of 500 nm has a collimated far-field pattern and is thus more suitable for the HMD system. The enhancement in optical efficiency can be increased up to 2.66 times and the normalized on-axis intensity for the pupil of the eyepiece can be increased up to 3.95 times. From the evaluation results of the HMD system, it can be seen that the 2nd pattern has the maximum LEE according to the FDTD method but the normalized on-axis intensity in the pupil of the eyepiece is even lower than that of conventional OLEDs. Although the enhancement of the LEE for the 3rd pattern is less than for the 2nd pattern, it is advantageous for the HMD system when the intensity distribution is collimated. These results indicate that the collimated far-field pattern is more important than the LEE enhancement when the OLED plane is used in an HMD system. At the same time, the collimated far-field pattern of the 10-fold QC OLEDs can be utilized in the HMD system to achieve power saving. There can be a reduction in the energy usage of the OLED panel of 74.68% while obtaining the same on-axis intensity for the pupil of the eyepiece as for conventional OLEDs. Therefore, the OLED with the 10-fold QC structure not only has a strong impact on the LEE but also offers a novel architecture for the HMD system.

Acknowledgments

This study was supported in part by the National Science Council, project numbers NSC102-2220-E-009-006 and NSC101-2622-E-009-CC3, and in part by the "Aim for the Top University Plan" of the National Chiao Tung University and the Ministry of Education, Taiwan, and the Ministry of Economic Affairs, R.O.C., under Grant No. D327HK2410.